Preparation of multistage microporous and mesoporous nitrogen-doped carbon nanospheres and study on electrocatalytic oxygen reduction

Houdong Rao[1], Shuxi Shan[2], Dongyang Zhang[3], Ling Zhang[4], Wenfei Wang[5]
Luoyang Ship Material Research Institute, Luoyang, 471023, China
[1]Corresponding author
E-mail: [1]*q8rao8@163.com*, [2]*1982171151@qq.com*, [3]*zdy_dut@163.com*, [4]*zhangling918813@163.com*, [5]*13783172546@163.com*

Check for updates

Abstract. Non-metallic carbon-based catalysts are one of the most promising catalysts for electrocatalytic oxygen reduction (ORR). However, the controlled synthesis of the pore structures of carbon-based catalysts and the determination of catalytic sites still remains to be further explored. Based on this, two nitrogen-doped carbon-based catalysts with microporous and mesoporous structures were prepared in this paper. The two catalysts had different pore structures and nitrogen-doped species. The experimental results showed that the carbon-based catalyst (PC-NH$_3$) rich in microporous structure and pyridine nitrogen doping had better catalytic performance, the electrocatalytic oxygen reduction performance of the catalyst was comparable to that of the platinum catalyst, and it had excellent methanol resistance and stability. This study provided important guidance for the application of porous carbon materials in oxygen reduction.

Keywords: microporous, nitrogen doped, carbon material, electrocatalyst, oxygen reduction.

1. Introduction

The technology of proton exchange membrane fuel cell could effectively alleviate the energy crisis and environmental pollution because of its high efficiency, green and clean advantages, which is an ideal alternative to fossil energy clean energy [1-2]. At present, the cathodic oxygen reduction catalysts for fuel cells are mainly precious metals such as Pt and Pd, and their alloys. Their high price greatly limits the large-scale industrial application of this technology [3-5]. Therefore, it is imperative to explore oxygen reduction catalysts with high activity, high stability, low cost and friendly environmental [6].

Non-metallic carbon-based catalysts have attracted extensive attention due to their advantages such as good conductivity, large specific surface area, abundant reserves and friendly environmental [7-9]. The controlled synthesis of pore structure and heteroatom doping are effective means to regulate carbon-based catalysts [10-12]. Usually, the hierarchical structure with pore size and pore volume composed of macropore, mesopore or micropore, which largely determines the kinetics of oxygen adsorption and diffusion [13]. In addition to the high surface area and controllable nanostructures, electrocatalysts also need good electron transfer conductivity, excellent activity and high chemical stability. Generally, doping nitrogen and other heteroatoms into the carbon matrix can regulate the local electronic structure of the carbon-based catalyst to improve the overall conductivity of the catalyst, and providing more active sites to enhance the interaction between carbon and oxygen molecules [14-19]. In carbon-based catalysts, the effects of macro-porous, mesoporous and microporous structures on oxygen adsorption and diffusion are different, and doping of different nitrogen species (pyridine nitrogen, graphite nitrogen, nitrogen oxide and etc.) has different effects on catalytic performance. However, up to now, the controlled synthesis of pore structure and precise doping of nitrogen species are still a major problem in the preparation of carbon-based catalysts [20-22].

Therefore, we developed a low concentration hydrothermal method to synthesize two nitrogen-doped spherical porous carbon-based catalysts. The two catalysts have different pore structures and nitrogen-doped species. The PC-NH$_3$ catalyst is rich in microporous structure and pyridine nitrogen doping, while the PC-N$_2$ catalyst is rich in mesoporous structure and graphite nitrogen doping. Performance tests show that, PC-NH$_3$ catalyst has better oxygen reduction performance, methanol resistance and stability. This indicates that compared with mesoporous structure and graphite nitrogen doping, the microporous structure and pyridine nitrogen doped carbon-based catalyst are more conducive to oxygen reduction reaction.

2. Experiment

2.1. Synthesis of catalyst

2.1.1. Laboratory reagents

Phenol, sodium hydroxide, formaldehyde, potassium hydroxide and Pt/C were purchased from Beijing Inokai Technology Co., LTD. Pluronic F127 (960 mg, Mw = 12600 g·mol^{-1}) and melamine were purchased from Alfa Esar (China) Chemical Co., LTD. Ammonia, nitrogen and oxygen were purchased from Beijing Telong Technology Co., LTD.

2.1.2. Sample preparation

Phenol (600 mg), aqueous formalin solution (3 mL, 37 wt.%) and NaOH aqueous solution (15 mL, 0.1 M) were mixed and heated at 70 °C for 1 h under intense stirring. Subsequently, melamine (100 mg) and Pluronic F127 (960 mg, Mw = 12600 g mol^{-1}) dissolved in 15 mL of deionized water was added. The resulting mixture was then stirred at 80 °C for 7 h. Subsequently, the solution was diluted with 60 mL of deionized water and then maintained at 70 °C for 24h under constant stirring. Then, 50 mL of the resulting solution and 150 mL of deionized water were transferred into a Teflon-lined stainless steel autoclave and heated at 130 °C for 24 h. The porous polymer nanospheres formed were collected by centrifugation and washed repeatedly with deionized water. The porous polymer nanospheres were then transformed to defective N-doped carbon spheres by heating at 1000 °C for 2 h under an NH$_3$ or N$_2$flow, marked as PC-NH$_3$ and PC-N$_2$, respectively.

2.2. Performance and characterization of samples

Morphology and elemental analysis of the samples were performed using a JEOL-2100F transmission microscope with an acceleration voltage of 200 kV. The method of characterization was to add the catalyst sample solution on the ultra-thin carbon film, then dried it fully and characterized it. X-ray photoelectron spectroscopy (XPS) data were acquired on a VGESCALABMKII X-ray photo-electron spectrometer equipped with a non-monochromatized Al-Kα X-ray source (hν = 1486.7 eV). Raman spectra were obtained on a Renishaw in Via-Reflex spectrometer system. The spectra were excited using a 532 nm source.

The electrocatalytic oxygen reduction performance was tested in a three-electrode system on an electrochemical workstation (CHI 760E). Method for preparing the working electrode: the 8 mg sample was dispersed in a solution of 500 uL deionized water and 460 uL ethanol, 40 uL nafion solution was added in it, and sonicated for 2 h. And then, 3 uL of the sample dispersed droplets were added to the glassy carbon electrode and dried thoroughly. Saturated Ag/AgCl electrode and platinum wire electrode were used as reference electrode and counter electrode, respectively.

3. Results and discussion

3.1. Characterization and analysis of surface structure

As a precursor of nitrogenous non-metallic carbon spheres, the nitrogenous polymer spheres were first synthesized. Polymer molecules were synthesized from phenol and formaldehyde through the phenol-formaldehyde condensation reaction. The nitrogenous polymer spheres were synthesized in the environment of melamine with the action of F127, as shown in Fig. 1(a). Nitrogen-containing polymer spheres were calcined and carbonized at high temperature under NH_3 or N_2 atmosphere to form samples PC-NH_3 (Fig. 1(b)) and PC-N_2 (Fig. 1(c)), respectively. It was obvious that the volume of a single sphere was significantly reduced after calcination, however, the spherical morphology was still maintained. The difference between PC-NH_3 and PC-N_2 could not be seen from the morphology alone. XPS was used to characterize the N content and N-doped species of the two catalysts, as shown in Fig. 2. The nitrogen contents of PC-NH_3 and PC-N_2 were 3.15 at% and 2.89 at%, respectively. The results were not that different, but the nitrogen content of the two species was very different, PC-NH_3 mainly contained pyridine nitrogen heteroatoms, while PC-N_2 mainly contained graphite nitrogen heteroatoms. This could be because NH_3 had an etching effect on carbon materials at high temperatures, the carbon material could be N-doped with its own N, and the N-doped form of the material itself was reconstructed [23-25].
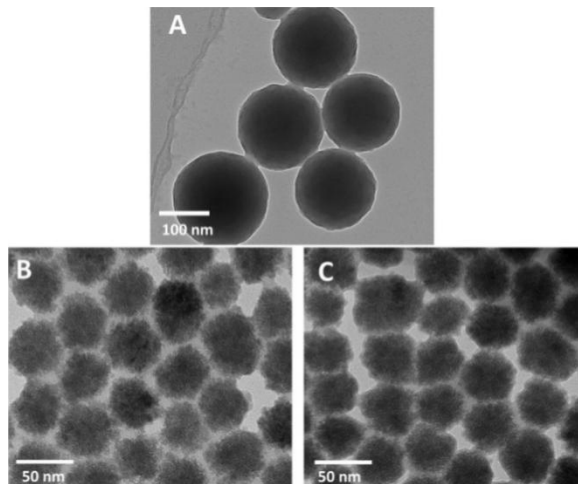

Fig. 1. a) TEM image of polymer spheres, b) TEM image of PC-N_2, c) TEM image of PC-NH_3
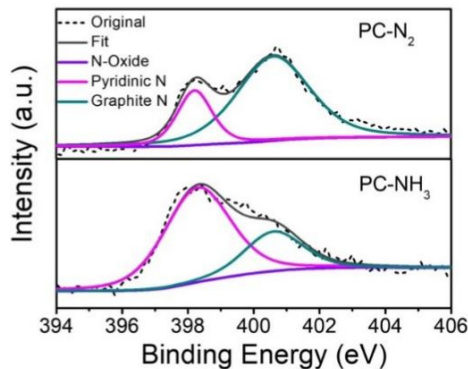

Fig. 2. N 1s of PC-N_2 and PC-NH_3

The specific surface area of carbon-based catalysts is an important index affecting the catalytic

performance of catalysts. Nitrogen adsorption and desorption isotherms of PC-N_2 and PC-NH_3 were shown in Fig. 3. It was obvious that the specific surface area of PC-N_2 (931 $m^2 \cdot g^{-1}$) was larger than that of PC-NH_3 (815 $m^2 \cdot g^{-1}$). This meant that the etching of ammonia caused the pore structure of the catalyst to change at high temperatures, it reduced the specific surface area of the catalyst. In addition to the specific surface area of the catalyst, the pore size distribution of the catalyst directly affected the diffusion and adsorption process of oxygen, and then it affected the catalytic performance of the catalyst. Pore size distribution curves for PC- N_2 and PC-NH_3 were shown in Fig. 4. It proved that the pore size distribution of the two catalysts was quite different. The amount of micropore in PC-NH_3 sample was significantly higher than that in PC-N_2 sample. However, the amount of mesopore in the former was much lower than that in the latter. This might be due to the etching of ammonia led to the collapse of the mesoporous structure of the material itself at high temperature, at the same time, the microporous structure with relatively small pores was formed.
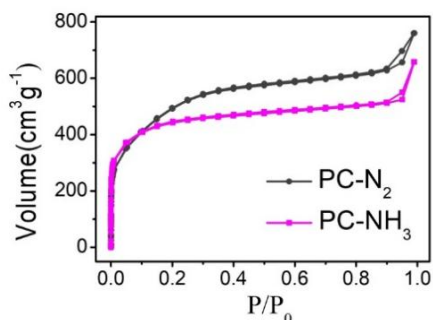

Fig. 3. Nitrogen adsorption and desorption isotherms for PC-N_2 and PC-NH_3

BET specific surface areas calculated from N_2 physisorption data were 931 $m^2 \cdot g^{-1}$ and 815 $m^2 \cdot g^{-1}$ for PC-N_2 and PC-NH_3, respectively.
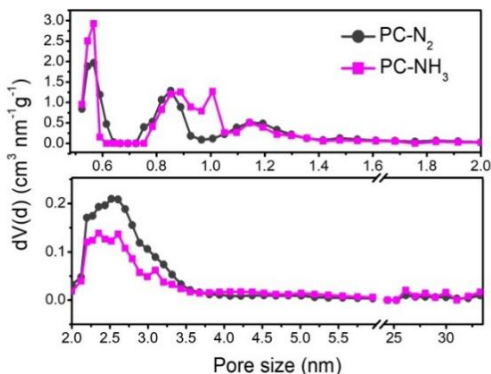

Fig. 4. Pore size distribution curves for PC-N_2 and PC-NH_3

Based on the above experimental data, we successfully synthesized two kinds of porous carbon-based non-metallic catalysts with different pore structures and nitrogen-doped species. The obvious differences of micro- and mesoporous structures and N-doped species were beneficial to explore the relationship between the structure and catalytic performance of catalysts, which was the basis for the study of catalytic reaction mechanism.

3.2. Characterization of catalytic properties of oxygen reduction

The catalytic performance of PC-N_2 and PC-NH_3 is shown in Fig. 5(a). The half-wave

potentials of oxygen reduction of PC-N_2 and PC-NH_3 samples were –0.185 V and –0.138 V (vs Ag/AgCl), respectively, the catalytic performance of the latter was significantly better than that of the former, and it was closed to the half-wave potential of Pt witch was –0.141 V (vs Ag/AgCl). Comprehensive analysis of structural characterization data, the PC-NH_3 samples with microporous structure and pyridine nitrogen doping had excellent catalytic performance. This indicated that the microporous structure and pyridine nitrogen were more conducive to oxygen reduction among the types of carbon-based catalysts. Pt-based catalysts have an obvious disadvantage, during the catalytic process, it was easy to be poisoned by methanol used in the battery, and the catalytic activity was greatly reduced. Therefore, we compared the methanol tolerance of PC-NH_3 and Pt, as shown in Fig. 5(b), PC-NH_3 had excellent methanol tolerance.
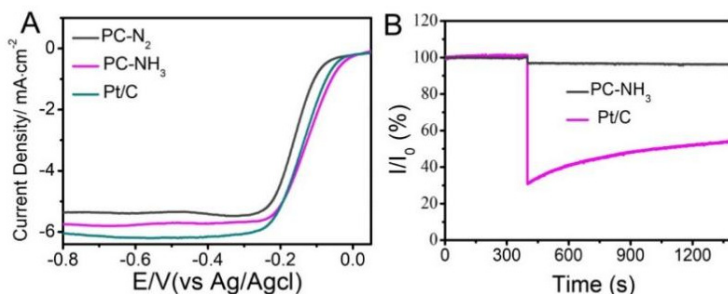

Fig. 5. a) LSV curves for PC- N_2, PC-NH_3 and Pt/C at an RDE rotation rate of 1600 rpm with a scan rate of 10 mV·s^{-1}, b) $I - t$ chronoamperometric responses for PC-NH_3 and Pt/C at 0.2 V and 1600 rpm with 5 % (v/v) methanol addition at around 1400 s, I_0 is the initial current

4. Conclusions

In this paper, nitrogen-containing polymer carbon spheres were synthesized by a low concentration hydrothermal method. Two spherical porous carbon-based catalysts with different pore structures and nitrogen-doped species were synthesized by the calcination of NH_3 and N_2 on polymers at high temperature. The results of structural characterization showed that the catalyst PC-NH_3 was rich in microporous structure and pyridine nitrogen doping, while PC-N_2 was rich in mesoporous structure and graphite nitrogen doping. The performance test results showed that PC-NH_3 had better oxygen reduction performance and methanol resistance. This meant that compared with carbon-based catalysts contained mesoporous structures and graphite nitrogen doping, the carbon-based catalyst with microporous structure and pyridine nitrogen doping was more conducive to oxygen reduction reaction. This work laid an important research foundation for exploring more excellent non-metallic carbon-based catalysts and had a certain guiding role.

Data availability

The datasets generated during and/or analyzed during the current study are available from the corresponding author on reasonable request.

Conflict of interest

The authors declare that they have no conflict of interest.

References

[1] Z. Peng, S. A. Freunberger, Y. Chen, and P. G. Bruce, "A reversible and higher-rate Li-O2battery," *Science*, Vol. 337, pp. 563–566, 2012, https://doi.org/10.1126/science.122398

[2] B. Dunn, H. Kamath, and J.-M. Tarascon, "Electrical Energy Storage for the Grid: A Battery of Choices," *Science*, Vol. 334, No. 6058, pp. 928–935, Nov. 2011, https://doi.org/10.1126/science.1212741

[3] L. Shang et al., "Well-Dispersed ZIF-Derived Co,N-Co-doped Carbon Nanoframes through Mesoporous-Silica-Protected Calcination as Efficient Oxygen Reduction Electrocatalysts," *Advanced Materials*, Vol. 28, No. 8, pp. 1668–1674, Feb. 2016, https://doi.org/10.1002/adma.201505045

[4] J. Oh, S. Park, D. Jang, Y. Shin, D. Lim, and S. Park, "Metal-free N-doped carbon blacks as excellent electrocatalysts for oxygen reduction reactions," *Carbon*, Vol. 145, pp. 481–487, Apr. 2019, https://doi.org/10.1016/j.carbon.2019.01.056

[5] Q. Xiang et al., "A study of defect-rich carbon spheres as a metal-free electrocatalyst for an efficient oxygen reduction reaction," *Journal of Materials Chemistry A*, Vol. 5, No. 46, pp. 24314–24320, 2017, https://doi.org/10.1039/c7ta07203a

[6] G. Ren et al., "N-doped porous carbon spheres as metal-free electrocatalyst for oxygen reduction reaction," *Journal of Materials Chemistry A*, Vol. 9, No. 9, pp. 5751–5758, Mar. 2021, https://doi.org/10.1039/d0ta11493f

[7] J. Zhang, Z. Zhao, Z. Xia, and L. Dai, "A metal-free bifunctional electrocatalyst for oxygen reduction and oxygen evolution reactions," *Nature Nanotechnology*, Vol. 10, No. 5, pp. 444–452, May 2015, https://doi.org/10.1038/nnano.2015.48

[8] T. Pan, H. Liu, G. Ren, Y. Li, X. Lu, and Y. Zhu, "Metal-free porous nitrogen-doped carbon nanotubes for enhanced oxygen reduction and evolution reactions," *Science Bulletin*, Vol. 61, No. 11, pp. 889–896, Jun. 2016, https://doi.org/10.1007/s11434-016-1073-3

[9] Q. Lv et al., "Selectively nitrogen-doped carbon materials as superior metal-free catalysts for oxygen reduction," *Nature Communications*, Vol. 9, No. 1, pp. 1–11, Dec. 2018, https://doi.org/10.1038/s41467-018-05878-y

[10] H.-W. Liang, W. Wei, Z.-S. Wu, X. Feng, and K. Müllen, "Mesoporous metal-nitrogen-doped carbon electrocatalysts for highly efficient oxygen reduction reaction," *Journal of the American Chemical Society*, Vol. 135, No. 43, pp. 16002–16005, Oct. 2013, https://doi.org/10.1021/ja407552k

[11] X. Wu et al., "Mesoporous hollow nitrogen-doped carbon nanospheres with embedded $MnFe_2O_4$/Fe hybrid nanoparticles as efficient bifunctional oxygen electrocatalysts in alkaline media," *ACS Applied Materials and Interfaces*, Vol. 10, No. 24, pp. 20440–20447, Jun. 2018, https://doi.org/10.1021/acsami.8b04012

[12] Y. Wang, H. Lv, L. Sun, and B. Liu, "Mesoporous noble metal-metalloid/nonmetal alloy nanomaterials: designing highly efficient catalysts," *ACS Nano*, Vol. 15, No. 12, pp. 18661–18670, Dec. 2021, https://doi.org/10.1021/acsnano.1c10112

[13] Y. Hu, X. Guo, T. Shen, Y. Zhu, and D. Wang, "Hollow porous carbon-confined atomically ordered $PtCo_3$ intermetallics for an efficient oxygen reduction reaction," *ACS Catalysis*, Vol. 12, No. 9, pp. 5380–5387, May 2022, https://doi.org/10.1021/acscatal.2c01541

[14] Y. Zhou et al., "Atomic Fe dispersed hierarchical mesoporous Fe-N-C nanostructures for an efficient oxygen reduction reaction," *ACS Catalysis*, Vol. 11, No. 1, pp. 74–81, Jan. 2021, https://doi.org/10.1021/acscatal.0c03496

[15] C. Ouyang, L. Zheng, Q. Zhang, and X. Wang, "A simple preheating-pyrolysis strategy leading to superior oxygen reduction reaction activity in Fe-N/carbon black," *Advanced Materials*, Vol. 34, No. 40, p. 2205372, Oct. 2022, https://doi.org/10.1002/adma.202205372

[16] B. Bayatsarmadi, Y. Zheng, M. Jaroniec, and S. Z. Qiao, "Soft-templating synthesis of N-doped mesoporous carbon nanospheres for enhanced oxygen reduction reaction," *Chemistry – An Asian Journal*, Vol. 10, No. 7, pp. 1546–1553, Jul. 2015, https://doi.org/10.1002/asia.201500287

[17] K. Wang, H. Chai, and Y. Cao, "using anion-exchange to induce the formation of edge defects in CoN_x to enhance ORR activity," *ChemCatChem*, Vol. 14, No. 13, Jul. 2022, https://doi.org/10.1002/cctc.202200146

[18] K. Gao et al., "Efficient metal-free electrocatalysts from N-doped carbon nanomaterials: mono-doping and co-doping," *Advanced Materials*, Vol. 31, No. 13, p. 1805121, Mar. 2019, https://doi.org/10.1002/adma.201805121

[19] S. K. Singh, K. Takeyasu, and J. Nakamura, "Active sites and mechanism of oxygen reduction reaction electrocatalysis on nitrogen-doped carbon materials," *Advanced Materials*, Vol. 31, No. 13, p. 1804297, Mar. 2019, https://doi.org/10.1002/adma.201804297

[20] B. Liu et al., "Metal-organic framework assembly derived hierarchically ordered porous carbon for oxygen reduction in both alkaline and acidic media," *Chemical Engineering Journal*, Vol. 430, p. 132762, Feb. 2022, https://doi.org/10.1016/j.cej.2021.132762

[21] Z. Xu, Z. Zhou, B. Li, G. Wang, and P. W. Leu, "Identification of efficient active sites in nitrogen-doped carbon nanotubes for oxygen reduction reaction," *The Journal of Physical Chemistry C*, Vol. 124, No. 16, pp. 8689–8696, Apr. 2020, https://doi.org/10.1021/acs.jpcc.9b11090

[22] H. Zhang et al., "Single atomic iron catalysts for oxygen reduction in acidic media: particle size control and thermal activation," *Journal of the American Chemical Society*, Vol. 139, No. 40, pp. 14143–14149, Oct. 2017, https://doi.org/10.1021/jacs.7b06514

[23] W. Wang et al., "Intrinsic carbon-defect-driven electrocatalytic reduction of carbon dioxide," *Advanced Materials*, Vol. 31, No. 19, p. 1808276, May 2019, https://doi.org/10.1002/adma.201808276

[24] J. Zhu and S. Mu, "Defect Engineering in carbon-based electrocatalysts: insight into intrinsic carbon defects," *Advanced Functional Materials*, Vol. 30, No. 25, p. 2001097, Jun. 2020, https://doi.org/10.1002/adfm.202001097

[25] X. Liu and L. Dai, "Carbon-based metal-free catalysts," *Nature Reviews Materials*, Vol. 1, No. 11, pp. 1–12, Nov. 2016, https://doi.org/10.1038/natrevmats.2016.64